

Reduced Cerebral Gray Matter and Altered White Matter in Boys with Duchenne Muscular Dystrophy

Nathalie Doorenweerd, MSc,^{1,2,3} Chiara S. Straathof, MD,³ Eve M. Dumas, PhD,³
 Pietro Spitali, PhD,⁴ Ieke B. Ginjaar, PhD,⁵ Beatrijs H. Wokke, MD,³
 Debby G. Schrans, MSc,⁶ Janneke C. van den Bergen, MD,³
 Erik W. van Zwet, PhD,⁷ Andrew Webb, PhD,¹ Mark A. van Buchem, MD, PhD,¹
 Jan J. Verschuuren, MD, PhD,³ Jos G. Hendriksen, PhD,^{6,8} Erik H. Niks, MD, PhD,³
 and Hermien E. Kan, PhD^{1,2}

Objective: Duchenne muscular dystrophy (DMD) is characterized by progressive muscle weakness caused by *DMD* gene mutations leading to absence of the full-length dystrophin protein in muscle. Multiple dystrophin isoforms are expressed in brain, but little is known about their function. DMD is associated with specific learning and behavioral disabilities that are more prominent in patients with mutations in the distal part of the *DMD* gene, predicted to affect expression of shorter protein isoforms. We used quantitative magnetic resonance (MR) imaging to study brain microstructure in DMD.

Methods: T1-weighted and diffusion tensor images were obtained on a 3T MR scanner from 30 patients and 22 age-matched controls (age = 8–18 years). All subjects underwent neuropsychological examination. Group comparisons on tissue volume and diffusion tensor imaging parameters were made between DMD patients and controls, and between 2 DMD subgroups that were classified according to predicted Dp140 isoform expression (DMD_Dp140⁺ and DMD_Dp140⁻).

Results: DMD patients had smaller total brain volume, smaller gray matter volume, lower white matter fractional anisotropy, and higher white matter mean and radial diffusivity than healthy controls. DMD patients also performed worse on neuropsychological examination. Subgroup analyses showed that DMD_Dp140⁻ subjects contributed most to the gray matter volume differences and performed worse on information processing.

Interpretation: Both gray and white matter is affected in boys with DMD at a whole brain level. Differences between the DMD_Dp140⁻ subgroup and controls indicate an important role for the Dp140 dystrophin isoform in cerebral development.

ANN NEUROL 2014;76:403–411

The X-linked disease Duchenne muscular dystrophy (DMD) is characterized by severe and progressive muscle weakness due to mutations in the *DMD* gene. Mutations cause the absence of dystrophin, a 427kDa protein.¹ Dystrophin provides structural stability by connecting the contractile filament actin and the dystrophin-

associated glycoprotein complex in the sarcolemma. In addition to muscle weakness, DMD is characterized by cognitive impairment that is thought to be nonprogressive. In patients, the mean full-scale intelligence quotient is approximately 1 standard deviation below normal.² DMD patients exhibit problems with verbal short-term

View this article online at wileyonlinelibrary.com. DOI: 10.1002/ana.24222

Received Apr 1, 2014, and in revised form Jul 8, 2014. Accepted for publication Jul 8, 2014.

Address correspondence to N. Doorenweerd, Leiden University Medical Center, Department of Radiology C-03-Q, Albinusdreef2, 2333 ZA Leiden, the Netherlands. E-mail: N.Doorenweerd@lumc.nl

From the ¹Department of Radiology, C. J. Gorter Center for High Field MRI, Leiden University Medical Center, Leiden; ²Leiden Institute for Brain and Cognition, Leiden; ³Department of Neurology, Leiden University Medical Center, Leiden; ⁴Department of Human Genetics, Leiden University Medical Center, Leiden; ⁵Department of Clinical Genetics, Leiden University Medical Center, Leiden; ⁶Department of Neurological Learning Disabilities, Kempenhaeghe Epilepsy Center, Heeze; ⁷Department of Medical Statistics, Leiden University Medical Center, Leiden; and ⁸Department of Neurology, Maastricht University Medical Center, Maastricht, the Netherlands..

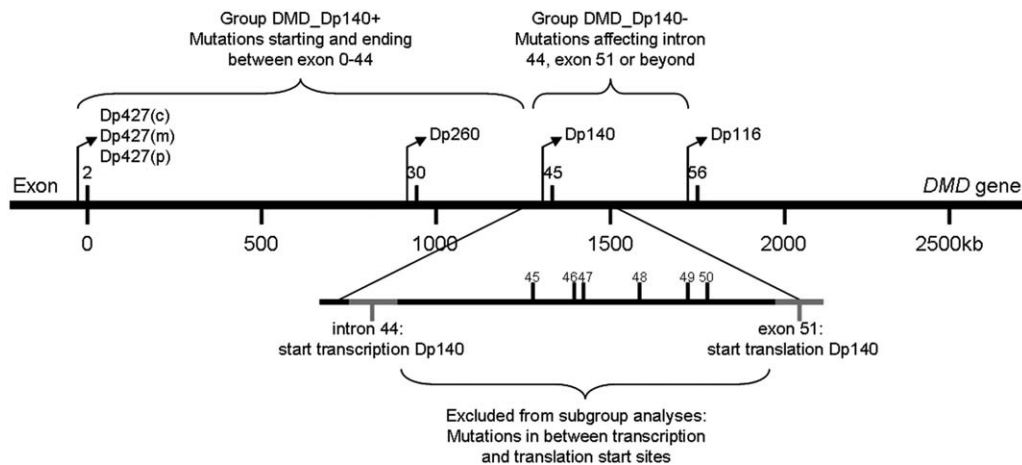


FIGURE 1: Dp140 transcription and translation sites used for subgroup classification. The prediction of Dp140 expression is based on mutation location in the *DMD* gene. There is a large gap between the start of transcription and start of translation for Dp140. Patients with a mutation starting and ending exactly in between transcription and translation were excluded from the analyses due to unpredictability of the mutation effect on Dp140 expression.

memory, visuospatial long-term memory, and verbal fluency.³ In addition, a higher incidence of autism spectrum disorders, attention deficit and hyperactivity disorders, and obsessive-compulsive disorders occurs, and specific learning disorders such as dyslexia have been described.⁴⁻⁶

In the central nervous system (CNS), full-length dystrophin (Dp427) is expressed mainly in cortical neurons and cerebellar Purkinje cells, but little is known about its function.⁷ At least 4 shorter isoforms of dystrophin are also present in the CNS, with molecular weights of 260, 140, 116, and 71kDa, respectively. These isoforms derive from alternative tissue-specific promoter sites that use the following exons as the N-terminal domain: exon 30 for Dp260, exon 45 for Dp140, exon 56 for Dp116, and exon 63 for Dp71.⁸ Cognitive impairment is more prominent in patients with mutations in the distal part of the *DMD* gene (downstream of exon 44) that are associated with the loss of Dp140 expression. This suggests a genotype-phenotype correlation between mutation and brain involvement.⁹

Postmortem studies of DMD patients have not shown consistent abnormalities.^{10,11} However, on a micro scale, architectural alterations in the cortical-spinal system and the parvalbumin- and calbindin-positive cortical circuitry have been found in a mouse model for DMD.¹²⁻¹⁴ Radiological studies in DMD patients showed glucose hypometabolism by positron emission tomography (PET) and altered metabolite concentrations by magnetic resonance spectroscopy.¹⁵⁻¹⁷ Magnetic resonance imaging (MRI) studies in DMD are limited to case reports and 1 quantitative study using voxel-based morphometry analysis and resting state functional MRI with a region of interest in the motor cortex.¹⁸ However,

quantitative information on in vivo whole brain morphology and microstructure in DMD is not available.

The aim of the present study was to investigate the brain in DMD using quantitative MRI to assess gray and white matter volume and microstructure. Composite scores for cognitive and behavioral functioning were analyzed in relation to MRI data. Finally, MRI data and composite scores were compared between 2 DMD subgroups with different mutations predicted to affect the expression of the Dp140 isoform and controls.

Subjects and Methods

Participants

DMD patients were recruited from the Dutch Dystrophinopathy Database, a nationwide patient registry. Exclusion criteria were the presence of MRI contraindications and the inability to lie supine for at least 30 minutes. DMD diagnosis had previously been confirmed using DNA extracted from whole blood taken from patients by a Gentra Puregene DNA purification kit (Gentra Systems, Minneapolis, MN), following the manufacturer's instructions. Deletion/duplication analysis of the *DMD* gene was performed using multiplex ligation-dependent probe amplification (MPLA kit Salsa P034/P035; MCR-Holland, Amsterdam, the Netherlands). Small mutations were identified by means of high-resolution melting curve analysis and subsequent sequence analysis.¹⁹ Within the recruited patients, 2 patient subgroups were distinguished (Fig 1). Patients carrying mutations upstream of intron 44 (transcription start site) were considered Dp140⁺. Patients with mutations involving exon 51 (translation start site) or the genomic region downstream of exon 51 were considered Dp140⁻. Deletions with 3' breakpoints in intron 44 were considered Dp140⁺ in case the breakpoint was upstream of the Dp140 promoter and unique first exon. A polymerase chain reaction (PCR)-based approach assessed whether the Dp140 promoter and first exon were

deleted using the forward primer Dp140F 5'-cttggcgaggcattg-3' and the reverse primer Dp140R3 5'-CCAGCTTTTAGGCA CACACA-3'. A second PCR was performed for these patients to confirm the presence of exon 51 using the forward primer hEx51F 5'-ggcttgacagaacttaccg-3' and the reverse primer h51r 5'-cttctgcttgatgatcatc-3'. Patients carrying deletions in the region between intron 44 and exon 51 were excluded due to the unpredictable effect on Dp140 expression. All protocols were approved by the local Medical Ethical Committee. All participants or their legal representatives provided written informed consent.

Procedures

The protocol was designed such that all tests could be performed on the same day. The Brooke scale for upper extremity function and Vignos scale for lower extremity function were used as measures of muscle function.²⁰ Participants were taken to a dummy scanner to familiarize themselves with the sounds and layout of an MRI machine. Subsequent neuropsychological evaluation (NPE) lasted a maximum of 1 hour. MRI scanning was then performed on a 3T scanner (Philips Achieva; Philips Healthcare, Best, the Netherlands) using an 8-channel receive-only head coil. Participants were placed supine with legs slightly elevated for comfort. Three-dimensional T1-weighted (T1w; echo time [TE] = 4.6 milliseconds, repetition time [TR] = 9.8 milliseconds, spatial resolution = $1.17 \times 0.92 \times 1.2$ mm, 4:55 minutes), T2-weighted (T2w; TE = 80 milliseconds, TR = 4,000 milliseconds, spatial resolution = $0.5 \times 0.46 \times 3.6$ mm, 2:46 minutes), fluid-attenuated inversion recovery (FLAIR; TE = 120 milliseconds, TR = 10,000 milliseconds, spatial resolution = $1 \times 0.8 \times 3.6$ mm, 4:00 minutes), and diffusion tensor (TE = 56 milliseconds, TR = 9,440 milliseconds, spatial resolution = $1.96 \times 2 \times 2$ mm, 32 directions, $b = 0$ and $1,000$ s/mm², 6:40 minutes) images were obtained parallel to the corpus callosum. An independent neuroradiologist assessed the scans for gross structural abnormalities and incidental findings.

Neuropsychology

Three composite scores were constructed using predefined parts of standardized and validated instruments reflecting the most important aspects of neuropsychological and behavioral/emotional functioning in DMD.²¹ The first composite score represented reading (scores standardized for age with range = 1–19, mean = 10, and standard deviation = 3 in healthy controls) and was based on the monosyllabic word reading test and the 1 minute reading test derived from CB&WL (“continu benoemen en woorden lezen”; Bos & Lutje Spelberg, Boom test uitgevers, Amsterdam, the Netherlands). The second composite score represented information processing (scores standardized for age with range = 1–19, mean = 10, and standard deviation = 3 in healthy controls), and used 2 subtests from the Kaufman Assessment Battery (number recall for auditory working memory and block counting for conceptual thinking) and 1 subtest from the Wechsler Intelligence Scale for Children (symbol search). The third composite score for emotional and behavioral

problems (range = 0–40) was constructed on the basis of the 4 problem-based subscales from the Dutch version of the Strengths and Difficulties Questionnaire for parents.²² The Personal Adjustment and Role Skills scale (PARS)-III, a parent report measure studied in 287 DMD patients, was used to assess psychosocial adjustment.²³ General intellectual level was assessed by the Peabody Picture Vocabulary test (PPVT-III-NL). This test measures receptive vocabulary, is normalized for age, and requires no motor response. It was previously used in 130 Duchenne boys.³

MRI

T1w and diffusion tensor imaging (DTI) scans were analyzed with FMRIB Software Library (FSL) software v5.0.²⁴ Intracranial volumes were obtained using the Brain Extraction Tool with BET2 + betsurf (BET v2.1)²⁵ and a fractional intensity threshold of 0.35. Gray matter, white matter, and cerebrospinal fluid (CSF) were segmented using the automated segmentation tool FAST.²⁶ Quantification of the volumes was performed with `fsstats -V` using the partial volume corrected output from FAST. DTI scans were corrected for motion and distortion using ExploreDTI.²⁷ ExploreDTI descriptive statistics were used to calculate mean whole brain fractional anisotropy (FA) and mean diffusivity (MD). Maps of axial diffusivity (AD), radial diffusivity (RD), FA, and MD were also created. These maps were then exported for tract-based spatial statistics (TBSS) in FSL.²⁸

Statistical Analysis

PARS and PPVT-III-NL scores of the DMD group were compared to known DMD populations using 1-sample *t* tests. One-sample *t* tests were also used to test volumetric differences in whole brain intracranial, white matter, gray matter, and CSF volumes, as well as NPE scores between patients and controls. To correct for multiple comparisons, we used the method of Benjamini and Hochberg, which limits the false discovery rate (FDR) to 5%.²⁹ One-way analysis of variance was used to assess differences in these same parameters between the subgroups DMD_Dp140⁺, DMD_Dp140⁻, and controls.

A univariate general linear model with Duchenne status of yes/no was used to assess the relation between 3 whole brain magnetic resonance (MR) measures decided upon before the analysis to reduce multiple comparisons (gray matter volume, mean FA, and mean MD) and the neuropsychological composite scores for each group, and to assess the relation between the whole brain MR measures and age. All analyses were performed using SPSS v20.0 (IBM, Armonk, NY) and considered significant at $p < 0.05$.

To localize MRI findings in specific areas of the brain, voxelwise statistical analyses were performed. For gray matter, voxel-based morphometry analysis (VBM) was performed with FSL-VBM.³⁰ For white matter, FA, MD, RD, and AD, data were analyzed with age as covariate using TBSS.²⁸ An additional TBSS analysis was performed with intracranial volume (ICV) and total brain volume (TBV) as covariates to assess the relationship between volume and white matter microstructure. The aligned maps from each subject were projected onto the FA skeleton, and the resulting data were used for voxel-wise cross-subject statistics

TABLE 1. Patient Characteristics and Available Assessments

Characteristic	Control	DMD	DMD_Dp140 ⁺	DMD_Dp140 ⁻
No. of participants	22	29	12	12
Age, yr ^a	13.1 (2.0)	12.3 (2.8)	13.1 (3.3)	12.0 (2.7)
Range, yr	8–16	8–18	9–18	8–16
Steroid treatment, No.	—	24	10	10
10 day on/10 day off cycle, No.	—	22	10	9
Brooke scale ^a	1	2.1 (1.6)	2.0 (1.6)	2.5 (1.7)
Vignos scale ^a	1	5.9 (3.1)	6.2 (3.1)	6.1 (3.2)
Wheelchair bound, No.	—	15	7	6
Age of loss of ambulation, yr ^a	—	10.2 (2.1)	11.0 (2.6)	9.9 (1.3)
Regular education, No.	22	17	8	6
Reading composite score, No.	21	25	11	12
Information composite score, No.	21	27	11	12
SDQ composite score, No.	22	28	11	12
3D T1 scans, No.	22	29	12	12
DTI scans, No.	21	25	10	10

^aData are presented as mean with standard deviation.
3D = 3-dimensional; DMD = Duchenne muscular dystrophy; DTI = diffusion tensor imaging. SDQ = Strengths and Difficulties Questionnaire, for emotional and behavioral problems

using Randomise, with 5000 permutations and threshold-free cluster enhancement (TCFE) to control for multiple comparison correction in each component separately with corrected probability of 0.05 determined as the significance threshold.³¹

Results

Participants

Thirty-three DMD boys (age = 8–18 years) and 22 healthy age-matched control boys (age = 8–16 years) participated in the study. Three DMD boys were excluded because they withdrew informed consent prior to the MRI scan ($n = 2$), or the scans could not be made due to technical problems ($n = 1$). In 5 DMD boys, 1 or more of the MRI scans could not be evaluated due to motion artifacts (1 T1w and 5 DTI), leaving 29 DMD boys for T1w analysis and 25 for DTI analysis. In the controls, 1 DTI scan was also excluded due to motion artifacts. Some NPE tests could not be completed within 1 hour prior to the MRI, resulting in the missing composite scores. Clinical characteristics and an overview of the available MRI and NPE assessments are summarized (Table 1). Representative T1w images are shown (Fig 2). DMD general intellectual level was not different from data reported in the literature using the PPVT-III (97.56 vs 98.15, respectively).³ Psychosocial adjustment, reflected by the PARS-III score, was significantly better than in historical controls

(91.62 vs 84.43, $p < 0.001$).²³ From the 29 DMD patients, 12 were classified as DMD_Dp140⁺ and 12 as DMD_Dp140⁻. Five DMD patients were excluded from the subgroup analysis because of the unpredictability of the mutation effect on Dp140 expression. No mutations downstream of exon 56 containing promoter sites of Dp116 and Dp71 were found.

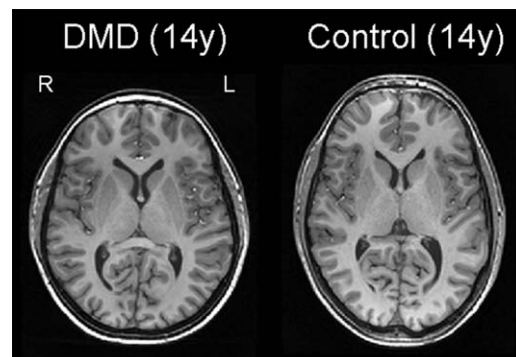


FIGURE 2: Representative T1-weighted images. A 14-year-old boy with Duchenne muscular dystrophy (DMD) is depicted on the left and an age-matched healthy control on the right. Images are displayed in the radiological convention with the left hemisphere on the right of the image. Note the absence of gross structural differences between the patient and the age-matched healthy control, which explains why routine visual assessment of the magnetic resonance images did not show abnormalities.

TABLE 2. Brain Structure Volumes in DMD Patients and Age-Matched Controls

Volumes	Control	DMD	DMD_Dp140 ⁺	DMD_Dp140 ⁻
Intracranial, cm ³	1,651 ± 95	1,584 ± 137	1,633 ± 149	1,550 ± 123
Total brain, cm ³	1,430 ± 78	1,355 ± 118 ^a	1,401 ± 121	1,324 ± 114 ^a
Grey matter, cm ³	811 ± 42	757 ± 56 ^b	770 ± 53	749 ± 63 ^b
White matter, cm ³	619 ± 45	598 ± 70	631 ± 75	576 ± 61
CSF, cm ³	222 ± 30	229 ± 32	232 ± 39	226 ± 29

^a $p < 0.05$
^b $p < 0.001$ after multiple comparison correction, significant differences between patient groups and controls.
 CSF = cerebrospinal fluid; DMD = Duchenne muscular dystrophy.

MRI

Visual assessment of the T1w, T2w, and FLAIR images did not reveal any gross structural brain abnormalities. Quantitative analysis of the T1w images showed a significantly smaller total brain and gray matter volume in DMD patients compared to controls (Table 2). Intracra-

nia volume was also smaller in DMD, although this difference failed to reach statistical significance ($p = 0.056$). Adding intracranial volume as a covariate in the analysis of gray matter and total brain volume showed that these structures were not smaller compared to total intracranial volume. VBM analysis showed small regions within the occipital cortex and the left insula that were significantly smaller in patients compared to controls (Fig 3A).

White matter FA was significantly lower in DMD in the occipital lobe (Fig 4). Significantly higher MD in DMD was found mainly in the corpus callosum. RD was significantly higher in DMD throughout the white matter. Taking ICV and TBV as covariates in the TBSS analysis revealed a relationship between these parameters and all 3 DTI measures, although part of the occipital lobe showed changes in FA and RD independent of volumetric parameters (data not shown).

DMD_Dp140⁻ patients had the smallest gray matter, total brain, and intracranial volumes (Fig 5A–C). VBM analysis showed differences between DMD_Dp140⁻ and controls in a different but similarly small area as found in the whole DMD group versus control analysis (Fig 3B). TBSS showed similar results for DMD_Dp140⁺ and DMD_Dp140⁻ versus control with significantly lower FA and higher RD, but no differences in MD. There was no effect of age on gray matter, white matter, or total brain volumes. However, age did correlate with white matter microstructure, with higher FA and lower MD and RD with increasing age.

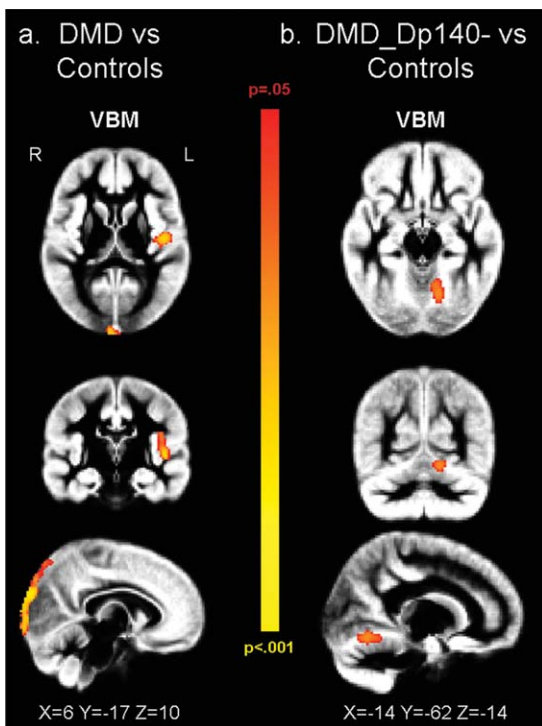


FIGURE 3: Gray matter voxel-based morphometry results. (A) Local gray matter reductions in part of the left insula and occipital lobe are demonstrated by voxel-based morphometry analysis (VBM) when comparing the whole patient group to controls. **(B)** Local gray matter reductions in part of the lingual gyrus and left cerebellar cortex are demonstrated by VBM when comparing the DMD_Dp140⁻ subgroup to controls. No differences were found between DMD_Dp140⁺ and controls (data not shown). Images are displayed in the radiological convention with the left hemisphere on the right side. DMD = Duchenne muscular dystrophy.

Neuropsychological Parameters

All 3 NPE composite scores were significantly different between DMD patients and controls, with DMD patients performing worse. Subgroup analysis showed that DMD_Dp140⁻ patients performed worst on all composite scores, although this difference was statistically significant only for information processing. Scores of

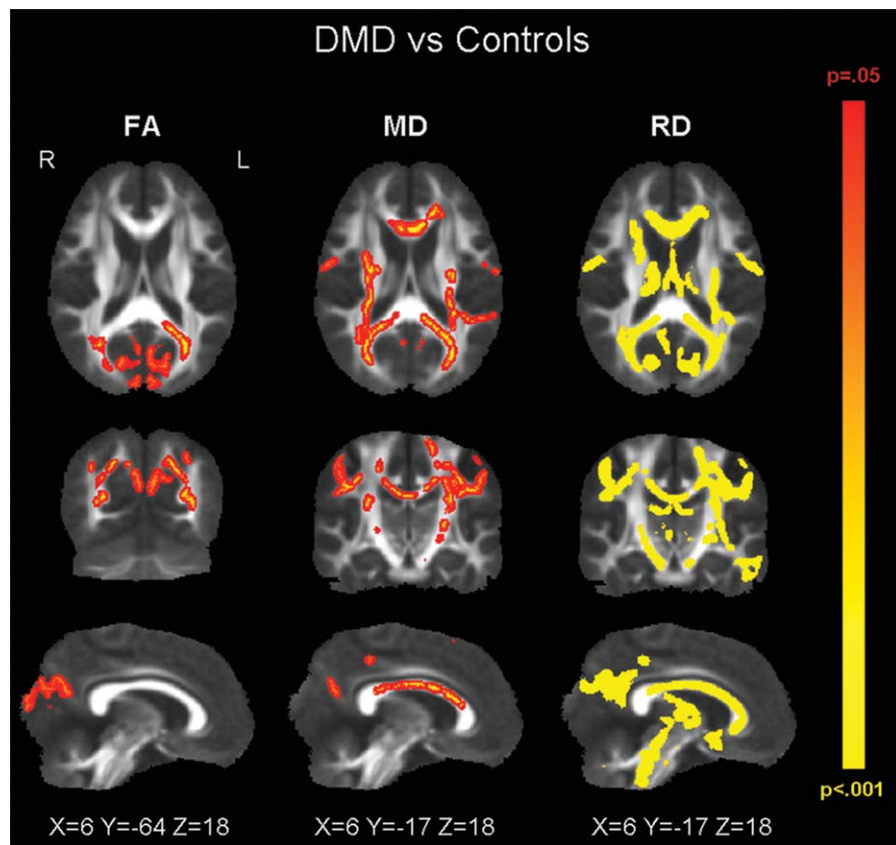


FIGURE 4: Diffusion tensor imaging analyses of the white matter. Widespread alterations in white matter with reduced fractional anisotropy (FA) in the occipital lobe, and increased mean diffusivity (MD) and radial diffusivity (RD) throughout are demonstrated by tract-based spatial statistics.

DMD_Dp140⁺ patients were between DMD_Dp140⁻ and controls (see Fig 5D–F). Within each subgroup, there were no significant correlations between the 3 composite scores and whole brain gray matter volume, whole brain FA, or whole brain MD using the univariate general linear model.

Discussion

In DMD patients, gray matter and total brain volume are smaller, and white matter microstructural integrity is altered compared to healthy age-matched controls. Strikingly, comparison of DMD patients with and without Dp140 expression with controls shows that DMD_Dp140⁻ patients, in whom the expression of the Dp140 isoform is predicted to be impaired, were more severely affected in terms of total brain and gray matter volumes as well as neuropsychological scores.

The smaller gray matter volume in DMD is global, as the regions in the occipital lobe and left insula identified by VBM are too small to account for the difference. This is in contrast to a previous quantitative MRI study in DMD brain, in which VBM identified a smaller volume in the left primary sensorimotor cortex, although no

analysis of absolute gray matter volumes was performed.¹⁸ One computed tomography study reported smaller gray matter volume in 20 of 30 DMD patients and contributed this difference to cortical atrophy. In the present study, skull size was proportional to total brain volume. There is a dynamic interaction between the developing brain and skull growth,^{32,33} with 25 to 27% increase in whole brain and intracranial volume between early childhood and adolescence. Therefore, correcting total brain volume with respect to intracranial volume enables the detection of atrophy. This implies that smaller brains in DMD are due to differences in maturation rather than atrophy.

In contrast to gray matter, white matter showed no difference in volume, but was significantly affected on a microstructural level as shown by DTI. The smaller FA and higher MD found in DMD indicate compromised structural complexity, and suggest reduced fiber density, increased membrane permeability, and/or decreased structural organization.³⁴ The higher RD in DMD indicates more fiber branching, decreased structural organization, or demyelination, which can lead to increased membrane permeability.^{35,36} The white matter microstructural

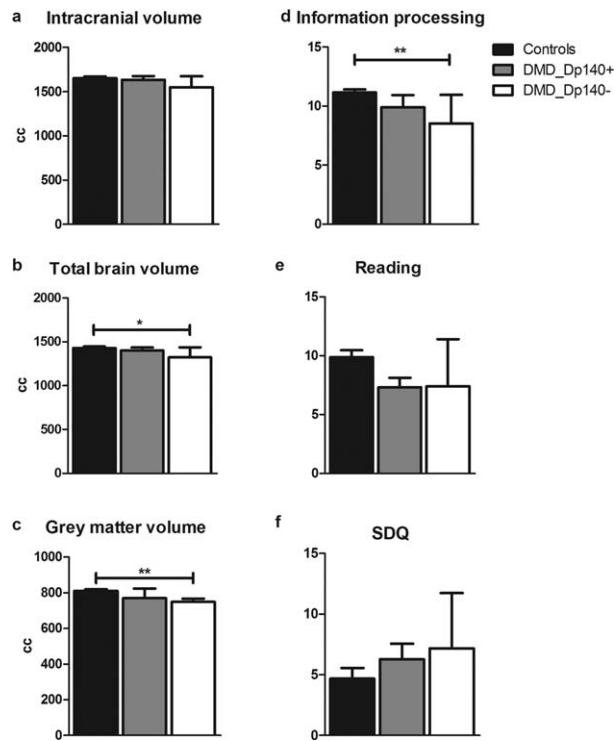


FIGURE 5: T1-weighted volumes and composite scores. Sub-group analyses are shown for controls (black) DMD_Dp140⁺ (gray), and DMD_Dp140⁻ (white). (A–C) Volumes (cc) of the intracranial (A), total brain (B), and gray matter (C) are depicted on the left. (D–F) Composite scores for information processing (D), reading (E), and emotional/behavioral problems derived from the Strengths and Difficulties Questionnaire (F; SDQ) are shown on the right. Significant differences between groups are indicated: * $p < 0.05$, ** $p < 0.01$ after multiple comparison correction.

differences between DMD and controls were associated with intracranial and total brain volume, although these cross-sectional data do not allow any conclusions regarding a causal relationship between the two. The global nature of the reduction in gray matter volume and microscopic nature of the white matter alterations could explain why these changes have not been described in previous post-mortem studies and conventional MRI studies, as they can only be observed with whole brain quantitative MRI.

The global reduction in gray matter volume of patients could be related to the finding that full-length Dp427, affected in all patients, is normally located in cortical and hippocampal pyramidal cells, the fetal cerebral cortex, and cerebellar Purkinje cells.⁷ In our DMD_Dp140⁻ subgroup, no mutations downstream of exon 56 were found. This implies that differences in MRI and NPE assessments in this study are mainly due to a lack of expression of the Dp140 isoform and do not include Dp116 and Dp71. The involvement of the Dp140 isoform in cognitive impairment was previously identified.⁹ Dp140 is predominantly active during fetal

development in the astroglial processes.⁷ DMD patients with mutations disturbing Dp71 expression were even more severely affected mentally.³⁷ Therefore, the loss of more dystrophin isoforms may well have a cumulative effect on altered brain maturation.

The correlation analyses did not reveal a significant association between mean whole brain gray matter volume, FA, or MD and the neuropsychological composite scores within the groups. A modest yet significant association between gray matter volume and total intelligence quotient was previously reported by Reiss et al³³ in 69 healthy children. Our study was not powered to find such function to morphology associations within the group of DMD patients or controls, but aimed at finding differences between these groups.

There are 2 potentially confounding issues in this study, which need to be specifically addressed. First, the brain still undergoes crucial developments in the age range of our subjects. Maximum global gray matter volume is reached between 6 and 9 years of age, after which it linearly declines approximately 5% per decade.³² White matter volume increases substantially from infancy through early adulthood with changes in myelination and axonal packing.³⁸ Age had a significant effect on FA, MD, and RD, which is in line with recent results.³⁸ This made a correction for age essential in the TBSS analysis despite matching for this parameter upon recruitment.

Second, the steroid treatment could have affected brain morphology. Volume reductions of hippocampus and amygdala have been observed in patients with asthma or rheumatic diseases receiving steroid treatment.³⁹ Children with excess endogenous glucocorticoids due to Cushing syndrome showed a significantly smaller total brain volume, larger ventricles, and smaller amygdala volumes than controls.⁴⁰ Five DMD patients in our study were steroid naive or had only been on steroid treatment for a short period of time at least 10 years before participating. Two of these patients were in DMD_Dp140⁺ and 2 in DMD_Dp140⁻. Given that DMD_Dp140⁻ showed the most extensive differences with controls in all tests, this strongly suggests that steroid use cannot be the main contributor to the morphological findings. However, a secondary contributing effect of the steroids on the morphological MRI findings cannot be excluded.

In conclusion, we observed significant global morphological and microstructural differences in the brain between DMD boys and controls. Results suggest that these differences arise from altered brain maturation rather than atrophy. Differences between DMD_Dp140⁺ and DMD_Dp140⁻ patients indicate an important role for the Dp140 dystrophin isoform in cerebral

development. Future studies could include longitudinal data to confirm the lack of atrophy or focus on assessment of the structural and functional connectivity between different brain networks (the connectome) and hopefully further dissect the role of each of the dystrophin brain isoforms.

Acknowledgment

The sponsors, Duchenne Parent Project NL and Gratama Stichting, had no role in study design, data collection, data analysis, data interpretation, or writing of the report.

The corresponding author had full access to all the data in the study and had final responsibility for the decision to submit for publication.

Authorship

The study was set up by C.S.S., H.E.K., J.J.V., J.G.H., E.H.N., and E.M.D.; participants were recruited by N.D. and C.S.S., aided by J.C.v.d.B.; N.D., H.E.K., D.G.S., E.M.D., and B.H.W. did the data acquisition; N.D., C.S.S., E.M.D., D.G.S., A.W., M.A.v.B., J.J.V., E.H.N., and H.E.K. were involved in the data discussion; genetic analyses were performed by P.S. and I.B.G.; statistical analyses were aided by E.W.v.Z.; data analyses and writing of the manuscript were performed by N.D.; editing of the manuscript was performed by H.E.K., E.H.N., J.G.H., and A.W.; the manuscript was reviewed by all authors.

Potential Conflicts of Interest

C.S.S.: trial support, Prosensa, GSK, Santhera; grants, Lilly, Duchenne Parent Project. J.J.V.: trial support, Prosensa, GSK, Santhera; grants, ZonMW, AFM, Lilly, Duchenne Parent Project; consultancy, Prosensa. E.H.N.: trial support, Prosensa, GSK, Santhera; grants, Lilly, Duchenne Parent Project. H.E.K.: grants, ZonMW, AFM, Duchenne Parent Project, Gratama Stichting; trial support, consultancy, Prosensa. All reimbursements were received by the Leiden University Medical Center. No personal financial benefits were received.

References

- Koenig M, Hoffman EP, Bertelson CJ, et al. Complete cloning of the Duchenne muscular dystrophy (DMD) cDNA and preliminary genomic organization of the DMD gene in normal and affected individuals. *Cell* 1987;50:509–517.
- Cotton SM, Voudouris NJ, Greenwood KM. Association between intellectual functioning and age in children and young adults with Duchenne muscular dystrophy: further results from a meta-analysis. *Dev Med Child Neurol* 2005;47:257–265.
- Cybulnik SE, Fee RJ, Batchelder A, et al. Cognitive and adaptive deficits in young children with Duchenne muscular dystrophy (DMD). *J Int Neuropsychol Soc* 2008;14:853–861.
- Hendriksen JG, Vles JS. Neuropsychiatric disorders in males with Duchenne muscular dystrophy: frequency rate of attention-deficit hyperactivity disorder (ADHD), autism spectrum disorder, and obsessive-compulsive disorder. *J Child Neurol* 2008;23:477–481.
- Hendriksen JGM, Vles JSH. Are males with Duchenne muscular dystrophy at risk for reading disabilities? *Pediatr Neurol* 2006;34:296–300.
- Wu JY, Kuban KCK, Allred E, et al. Association of Duchenne muscular dystrophy with autism spectrum disorder. *J Child Neurol* 2005;20:790–795.
- Lidov HG, Byers TJ, Watkins SC, et al. Localization of dystrophin to postsynaptic regions of central nervous system cortical neurons. *Nature* 1990;348:725–728.
- Feener CA, Koenig M, Kunkel LM. Alternative splicing of human dystrophin mRNA generates isoforms at the carboxy terminus. *Nature* 1989;338:509–511.
- Felisari G, Boneschi FM, Bardoni A, et al. Loss of Dp140 dystrophin isoform and intellectual impairment in Duchenne dystrophy. *Neurology* 2000;55:559–564.
- Dubowitz V, Crome L. The central nervous system in Duchenne muscular dystrophy. *Brain* 1969;92:805–808.
- Jagadha V, Becker LE. Brain morphology in Duchenne muscular dystrophy: a Golgi study. *Pediatr Neurol* 1988;4:87–92.
- Sbriccoli A, Santarelli M, Carretta D, et al. Architectural changes of the cortico-spinal system in the dystrophin defective mdx mouse. *Neurosci Lett* 1995;200:53–56.
- Carretta D, Santarelli M, Sbriccoli A, et al. Spatial analysis reveals alterations of parvalbumin- and calbindin-positive local circuit neurons in the cerebral cortex of mutant mdx mice. *Brain Res* 2004;1016:1–11.
- Carretta D, Santarelli M, Vanni D, et al. Cortical and brainstem neurons containing calcium-binding proteins in a murine model of Duchenne's muscular dystrophy: selective changes in the sensorimotor cortex. *J Comp Neurol* 2003;456:48–59.
- Lee JS, Pfund Z, Juhasz C, et al. Altered regional brain glucose metabolism in Duchenne muscular dystrophy: a pet study. *Muscle Nerve* 2002;26:506–512.
- Kreis R, Wingeier K, Vermathen P, et al. Brain metabolite composition in relation to cognitive function and dystrophin mutations in boys with Duchenne muscular dystrophy. *NMR Biomed* 2011;24:253–262.
- Rae C, Scott RB, Thompson CH, et al. Brain biochemistry in Duchenne muscular dystrophy: a 1H magnetic resonance and neuropsychological study. *J Neurol Sci* 1998;160:148–157.
- Lv SY, Zou QH, Cui JL, et al. Decreased gray matter concentration and local synchronization of spontaneous activity in the motor cortex in Duchenne muscular dystrophy. *AJNR Am J Neuroradiol* 2011;32:2196–2200.
- Almomani R, van der Stoep N, Bakker E, et al. Rapid and cost effective detection of small mutations in the DMD gene by high resolution melting curve analysis. *Neuromuscul Disord* 2009;19:383–390.
- Brooke MH, Fenichel GM, Griggs RC, et al. Clinical investigation of Duchenne muscular dystrophy. Interesting results in a trial of prednisone. *Arch Neurol* 1987;44:812–817.
- Snow WM, Anderson JE, Jakobson LS. Neuropsychological and neurobehavioral functioning in Duchenne muscular dystrophy: a review. *Neurosci Biobehav Rev* 2013;37:743–752.
- Goodman A, Goodman R. Strengths and difficulties questionnaire as a dimensional measure of child mental health. *J Am Acad Child Adolesc Psychiatry* 2009;48:400–403.

23. Hendriksen JG, Poysky JT, Schrans DG, et al. Psychosocial adjustment in males with Duchenne muscular dystrophy: psychometric properties and clinical utility of a parent-report questionnaire. *J Pediatr Psychol* 2009;34:69–78.
24. Smith SM, Jenkinson M, Woolrich MW, et al. Advances in functional and structural MR image analysis and implementation as FSL. *Neuroimage* 2004;23(suppl 1):S208–S219.
25. Smith SM. Fast robust automated brain extraction. *Hum Brain Mapp* 2002;17:143–155.
26. Zhang Y, Brady M, Smith S. Segmentation of brain MR images through a hidden Markov random field model and the expectation-maximization algorithm. *IEEE Trans Med Imaging* 2001;20:45–57.
27. Leemans A, Jeurissen B, Sijbers J, et al. ExploreDTI: a graphical toolbox for processing, analyzing, and visualizing diffusion MR data. *Proc Int Soc Mag Reson Med* 2009;17:3536 (Abstract).
28. Smith SM, Jenkinson M, Johansen-Berg H, et al. Tract-based spatial statistics: voxelwise analysis of multi-subject diffusion data. *Neuroimage* 2006;31:1487–1505.
29. Benjamini Y, Hochberg Y. Controlling the false discovery rate—a practical and powerful approach to multiple testing. *J R Stat Soc Series B Stat Methodol* 1995;57:289–300.
30. Good CD, Johnsrude IS, Ashburner J, et al. A voxel-based morphometric study of ageing in 465 normal adult human brains. *Neuroimage* 2001;14:21–36.
31. Bullmore ET, Suckling J, Overmeyer S, et al. Global, voxel, and cluster tests, by theory and permutation, for a difference between two groups of structural MR images of the brain. *IEEE Trans Med Imaging* 1999;18:32–42.
32. Courchesne E, Chisum HJ, Townsend J, et al. Normal brain development and aging: quantitative analysis at in vivo MR imaging in healthy volunteers. *Radiology* 2000;216:672–682.
33. Reiss AL, Abrams MT, Singer HS, et al. Brain development, gender and IQ in children. A volumetric imaging study. *Brain* 1996; 119(pt 5):1763–1774.
34. Assaf Y, Pasternak O. Diffusion tensor imaging (DTI)-based white matter mapping in brain research: a review. *J Mol Neurosci* 2008; 34:51–61.
35. Vandermosten M, Boets B, Wouters J, et al. A qualitative and quantitative review of diffusion tensor imaging studies in reading and dyslexia. *Neurosci Biobehav Rev* 2012;36:1532–1552.
36. Song SK, Yoshino J, Le TQ, et al. Demyelination increases radial diffusivity in corpus callosum of mouse brain. *Neuroimage* 2005; 26:132–140.
37. Moizard MP, Toutain A, Fournier D, et al. Severe cognitive impairment in DMD: obvious clinical indication for Dp71 isoform point mutation screening. *Eur J Hum Genet* 2000;8:552–556.
38. Lebel C, Walker L, Leemans A, et al. Microstructural maturation of the human brain from childhood to adulthood. *Neuroimage* 2008; 40:1044–1055.
39. Brown ES, Woolston DJ, Frol AB. Amygdala volume in patients receiving chronic corticosteroid therapy. *Biol Psychiatry* 2008;63: 705–709.
40. Coburn-Litvak PS, Tata DA, Gorby HE, et al. Chronic corticosterone affects brain weight, and mitochondrial, but not glial volume fraction in hippocampal area CA3. *Neuroscience* 2004;124:429–438.